Characterization of phospholipid mixed micelles by translational diffusion

James J. Chou[a], James L. Baber[b] & Ad Bax[b,*]
[a]*Department of Biological Chemistry & Molecular Pharmacology, Harvard Medical School, Boston, MA 02115, U.S.A.;* [b]*Laboratory of Chemical Physics, National Institute of Diabetes and Digestive and Kidney Diseases, National Institutes of Health, Bethesda, MD 20892, U.S.A.*

Abstract

The concentration dependence of the translational self diffusion rate, D_s, has been measured for a range of micelle and mixed micelle systems. Use of bipolar gradient pulse pairs in the longitudinal eddy current delay experiment minimizes NOE attenuation and is found critical for optimizing sensitivity of the translational diffusion measurement of macromolecules and aggregates. For low volume fractions Φ ($\Phi \leq 15\%$ v/v) of the micelles, experimental measurement of the concentration dependence, combined with use of the $D_s = D_o(1-3.2\lambda\Phi)$ relationship, yields the hydrodynamic volume. For proteins, the hydrodynamic volume, derived from D_s at infinitely dilute concentration, is found to be about 2.6 times the unhydrated molecular volume. Using the data collected for hen egg white lysozyme as a reference, diffusion data for dihexanoyl phosphatidylcholine (DHPC) micelles indicate approximately 27 molecules per micelle, and a critical micelle concentration of 14 mM. Differences in translational diffusion rates for detergent and long chain phospholipids in mixed micelles are attributed to rapid exchange between free and micelle-bound detergent. This difference permits determination of the free detergent concentration, which, for a high detergent to long chain phospholipid molar ratio, is found to depend strongly on this ratio. The hydrodynamic volume of DHPC/POPC bicelles, loaded with an M2 channel peptide homolog, derived from translational diffusion, predicts a rotational correlation time that slightly exceeds the value obtained from peptide ^{15}N relaxation data.

Introduction

Solution NMR is particularly well suited for the structural study of lipophilic peptides and small proteins that can be solubilized by a range of detergents. Traditionally, sodium dodecylsulfate (SDS) and dodecylphosphocholine (DPC) have been the detergents of choice, but more recently dihexanoylphosphatidylcholine (DHPC) is also finding increased use as a mild, zwitterionic detergent (Fernandez et al., 2002). However, the strong surface curvature of micelles has been suggested to induce strain in proteins interacting with the membrane surface, and the use of mixed micelles or bicelles has been proposed to present a more natural environment for

such systems (Vold et al., 1997; Chou et al., 2002). Mixed micelles used in biomolecular NMR consist of long-chain phospholipids, most commonly dimyristoylphosphatidylcholine (DMPC), and detergent (frequently DHPC). At low molar ratios, q, of long-chain phospholipid over detergent, the bicelles are disk-shaped with a radius that depends on q (Lin et al., 1991; Vold and Prosser, 1996; Glover et al., 2001; Luchette et al., 2001), whereas at high q values (q $\geq$ 2.5) and above the DMPC melting temperature (298 K) the bicelles aggregate edgewise to adopt a highly porous α-lamellar bilayer morphology (Gaemers and Bax, 2001; Nieh et al., 2001). Spectra of lipophilic peptides anchored to small bicelles can exhibit remarkably good resolution, despite the substantial sizes calculated for the bicelle-peptide aggregate (Vold et al., 1997; Chou et al., 2002), raising the

*To whom correspondence should be addressed. E-mail: bax@nih.gov

question to what extent the mobility of such peptides relative to the bicelle increases spectral resolution.

Here, we characterize the size of bicelles and micelles by pulsed field gradient (PFG) NMR, which is a proven tool for quantitative measurement of translational diffusion. Its usage has increased considerably over the past decade with the introduction of reasonably linear, self-shielded gradient coils in high resolution NMR probes. This makes it relatively straightforward to obtain quantitative translational diffusion constants for a wide variety of molecules, ranging from the solvent itself to large particles or aggregates, such as bicelles. These data, extrapolated to infinite dilution, not only provide the hydrodynamic size for the particle but, as we demonstrate here, the concentration dependence of the translational diffusion rate also provides a measure for the interaction volume, plus allows accurate measurement of the partitioning of free and micelle-bound detergent.

We apply these diffusion methods to study several different detergents and mixed micelles that recently have gained popularity in biomolecular NMR, including DHPC and lysolipid micelles, various DHPC/DMPC and DHPC/POPC bicelles, and an M2 channel peptide anchored in DHPC/POPC bicelles. For the latter, the rotational correlation time of the peptide, derived from ^{15}N relaxation, is found to be slightly longer than the value predicted on the basis of the volume derived from translational diffusion.

Experimental

Materials

DHPC (1,2-Dicaproyl-sn-Glycero-3-Phosphocholine), DMPC (1,2-Dimyristoyl-sn-Glycero-3-Phosphocholine), DMPS (1,2-Dimyristoyl-sn-Glycero-3-[Phospho-L-Serine]), POPC (1-Palmitoyl-2-Oleoyl-sn-Glycero-3-Phosphocholine), POPG (1-Palmitoyl-2-Oleoyl-sn-Glycero-3-[Phospho-rac-(1-glycerol)]), 16:0 Lyso PG (1-Palmitoyl-2-Hydroxy-sn-Glycero-3-[Phospho-rac-(1-glycerol)]) were all purchased from Avanti Polar Lipids and used as received. Hen egg white lysozyme was obtained from Sigma, dialyzed against distilled water, and subsequently lyophilized. A peptide mimicking the transmembrane region of the M2 channel protein of the *Influenza A* virus, with amino acid sequence SSPLVV-(^{15}N)A-ASII-(^{15}N)G-ILHLILWILDRL was synthesized by California Peptide Research, Inc. (Napa, CA).

NMR sample preparation

Reference lysozyme samples were prepared at concentrations of 120, 80, 40 and 8 mg/ml in 90% H_2O, 10% D_2O, 20 mM Na acetate, pH 4.3, with concentrations determined using $OD_{280} = 2.63$ mg^{-1} cm^{-1} ml (Knubovets et al., 1999).

All micelle and bicelle samples were prepared in 20 mM phosphate buffer, pH 6.5, 90% H_2O, 10% D_2O, 5 mM azide. Each bicelle solution was generated by first preparing a concentrated stock solution of DHPC in buffer. An appropriate amount of this stock solution was added to a weighted amount of lipid, followed by thorough mixing until all lipid was dissolved and the solution was completely clear. The bicelle mixture was used to solubilize the M2 peptide (in powder form), using repeated vortexing and centrifugation. The final sample contained 0.7 mM peptide and 200 mg/ml DHPC/POPC bicelles, and was equilibrated for 14 h at 37 °C, prior to NMR measurements. The sample was stepwise diluted to study the concentration dependence of the translational and rotational diffusion rates. In order to restrict the sample volume to the region over which the field gradients are most linear, all experiments were carried out in Shigemi microcells (Shigemi Inc., Allison Park, PA), with the sample length adjusted to 14.0 mm for all samples.

NMR experiments

All spectra were recorded on a Bruker DMX-600 NMR spectrometer operating at a ^{1}H frequency of 600 MHz, containing a QXI quadruple-resonance (^{1}H, ^{31}P, ^{13}C, ^{15}N) probehead with self-shielded pulsed field gradients in the x, y, and z directions. The gradients were calibrated at 25 °C on the residual ^{1}H signal in a sample of 99.9% D_2O, using the published value of $1.902 \pm 0.002 \times 10^{-9}$ m^2 s^{-1} for the self-diffusion coefficient of HDO at 25 °C (Mills, 1973; Holz and Weingartner, 1991; Price, 1997). The gradient strengths were found to be 66.7, 50.1, and 48.9 G/cm at the maximum current for the z, y, and x gradient coils, respectively. Diffusion measurements of all micelle and bicelle samples were carried out at 27 °C, using the BPP-LED experiment (Figure 1b) (Wu et al., 1995). While fixing the gradient duration δ at 4.8 ms, the diffusion delay T at 200 ms, and τ at 0.2 ms, the strength of the two pairs of 2.4 ms bipolar square gradients was increased stepwise and simultaneously in both the x and z directions.

For the mixed micelle samples, DHPC alkyl methyl signals (0.89 ppm) were sufficiently separated
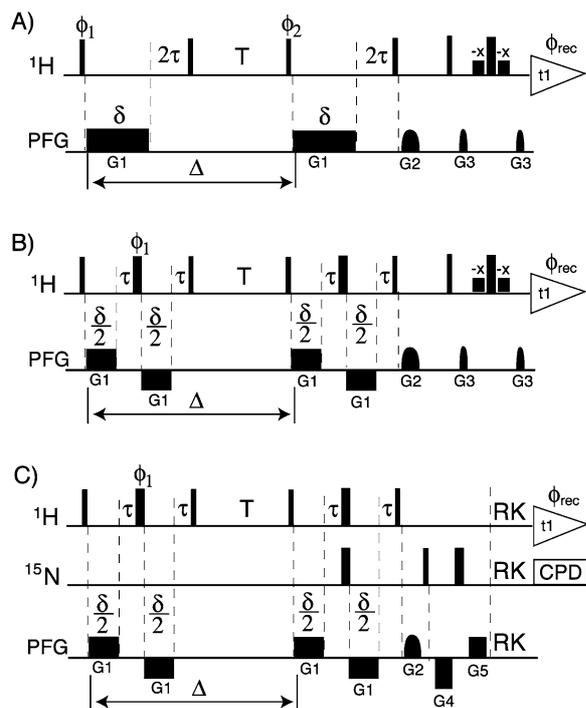
Figure 1. Pulse schemes of the LED diffusion experiments employed in this study. Narrow and wide pulses correspond to flip angles of 90° and 180° respectively. All pulse phases are x, unless specified otherwise. (A) Conventional Watergate-LED experiment. (B) Watergate BPP-LED experiment in which the single encoding or decoding gradient pulse in (A) is split into a pair of bipolar gradient pulses. (C) ^{15}N-edited BPP-LED experiment with Rance-Kay (RK) coherence selection as the readout element. In all three pulse schemes used for diffusion measurements, $\delta = 4.8$ ms, $\tau = 0.2$ ms, and T = 200 ms. The G1 rectangular pulsed field gradients are applied in the xz direction, at variable strength (see text). G2 is sine-bell shaped with a peak amplitude of 25 G/cm, 1.2 ms in duration, applied along the z axis. The Watergate gradient G3 is also sine-bell shaped, with a peak amplitude of 20 G/cm, and applied along the y axis. The rectangular encoding gradients in (C) have durations of 1 ms (G4, -z) and 0.7 ms (G5, z), with corresponding decoding gradients in the Rance-Kay read-out element 10-fold shorter. Phase cycling: (A) $\phi1 = $ x,−x,x,−x,y,−y,y,−y, $\phi2$ = x,x,−x,−x,y,y,−y,−y, and ϕ_{rec} = 2(x,−x,−x,x); (B,C) $\phi1$ = x,y,−x,−y, ϕ_{rec} = x,−x,x,−x.

from those of DMPC and POPC (0.84 ppm) to permit determination of their individual diffusion rates, without recourse to isotopic labeling.

The translational self diffusion coefficient D_s is obtained from the least-squares linear fit of

$$\ln[I(f)/I(f_0)] = -(\gamma\delta G_{max})^2(f^2 - f_0^2)(\Delta - \delta/3 - \tau/2)D_s, \tag{1}$$

where $I(f)$ is the intensity of the NMR signal as a function of the fractional gradient strength, f, which
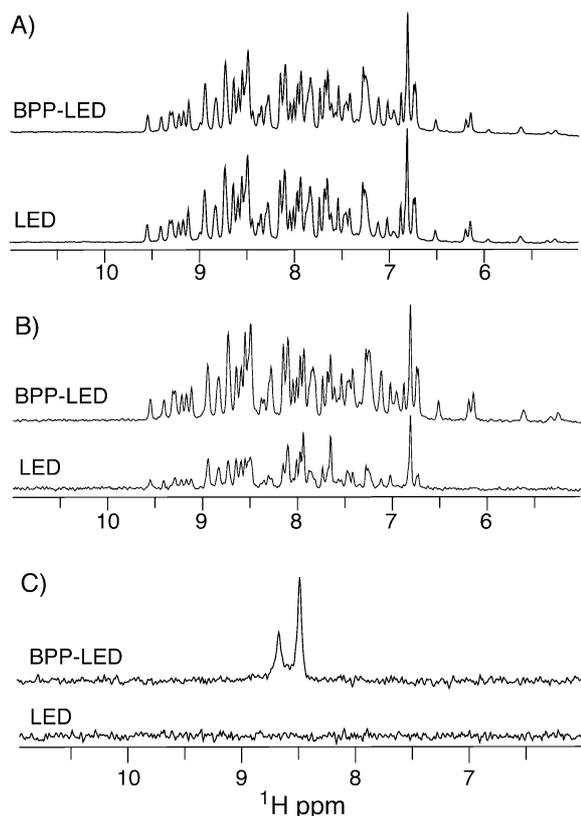
Figure 2. Comparison of signal strength recorded in regular LED and BPP-LED diffusion experiments. Attenuation in the regular LED experiment versus the BPP-LED experiment results from the [1]H-^{1}H NOE during the diffusion delay period, T. (A) spectra recorded for a sample of ubiquitin using $\delta = 4.8$ ms, $\tau = 0.2$ ms, G1: 3.2 G/cm in z; 2.4 G/cm in x, T = 3 ms; (B) same as (A) except T = 400 ms. (C) ^{15}N-edited version of the BBP-LED and LED experiments, recorded for A7 and G12 of 0.5 mg of M2 peptide reconstituted in 280 μl POPC/DHPC (q = 0.15; 200 mg/ml) bicelles; conditions are the same as in (A) except T = 300 ms.

is incremented from 0.05 to 0.45 in steps of 0.05, f_0 is the fractional gradient strength of the reference spectrum (0.02), γ is the gyromagnetic ratio of ^{1}H, G_{max} is the combined maximum gradient strength (82.7 G/cm) offered by the x and z gradient coils at $f = 1$. The delays Δ, δ, and τ are marked in Figure 1. In order to minimize the effect of gradient non-linearity, all gradient decay curves (including that of the HDO reference measurement) were measured over a gradient range that caused a maximum attenuation by about a factor 20.

The rotational diffusion correlation time, τ_c, of the M2 peptide in bicelles is obtained from the ratio of the [15]N T_1 and T_2 relaxation rates for both A7 and G12,
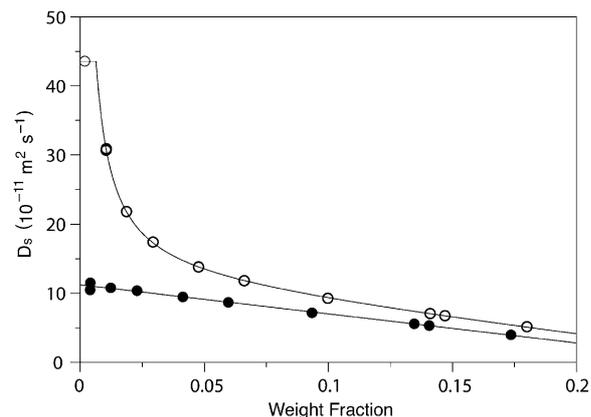
Figure 3. Concentration dependence of the experimentally observed DHPC self diffusion constant, D_s. Open circles are the measured D_s values, prior to correction for the diffusion contribution from free DHPC. Filled circles represent the diffusion coefficient of DHPC in micellar form (D_m), after correction for free DHPC (using Eqs 5 and 6). Linearity of the concentration dependence is optimal for [DHPC]$_{free}$ = 14 mM. So, for the filled circles, the horizontal axis represents the weight fraction of the DHPC micelles, not the total DHPC, which is 6.4×10^{-3} higher. For DHPC concentrations above the critical micelle concentration, open circles are fitted to $D_s = D_0[1 + \alpha(W_{total} - W_f)](W_{total} - W_f)/W_{total} + D_f W_f/W_{total}$, where W_{total} and W_f are respectively the weight fraction of all DHPC and the 14 mM free, monomeric DHPC. The data point represented by the left-most open circle corresponds to 5 mM DHPC and is not included in the fit since the diffusion coefficient of DHPC below the critical micelle concentration is constant.
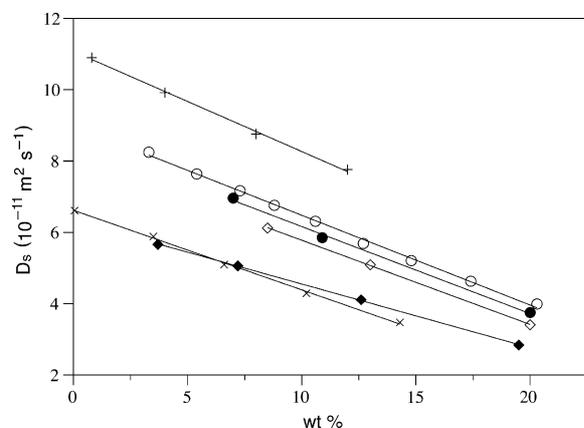
Figure 4. Experimental D_s values as a function of concentration (in weight fraction) for various samples of bicelles, micelles, and hen egg white lysozyme. The symbol representations are: (+) – lysozyme; (○) – POPC/DHPC bicelle (q = 0.15); (●) – POPC/DHPC bicelle (q = 0.15) with M2 peptide; (◇) – POPC/DHPC bicelle (q = 0.3) with M2 peptide; (◆) – POPC/DHPC bicelle (q = 0.53); (×) – 16:0 Lyso PG.

measured using standard T_1 and $T_{1\rho}$ experiments (Kay et al., 1992b; Korzhnev et al., 2002).

Results and discussion

Measurement of macromolecular diffusion

Quantitative measurement of the translational diffusion coefficient (D_s) by pulsed field gradient (PFG) NMR initially was based on a simple gradient echo experiment (Stejskal and Tanner, 1965), which puts stringent demands on gradient recovery. For the application to macromolecules with small translational diffusion coefficients ($D_s \sim 10^{-10}$ m²/s), the experiment requires the use of strong gradients and long diffusion delays between gradient pulses, during which signal decays as a result of rapid transverse relaxation. The stimulated echo experiment ($90° - \text{PFG}_{encode} - 90° - T_{diffusion} - 90° - \text{PFG}_{decode} - \text{Acquire}$) overcomes the transverse relaxation problem by separating the encoding and decoding PFG pulses by a time, $T_{diffusion}$, during which magnetization is stored along the z axis of the magnetic field (Tanner, 1970). During this storage time, the magnetization relaxes at a rate determined by the longitudinal, not the transverse relaxation time.

A further improvement by Gibbs and Johnson (1991) solves the gradient recovery problem by inserting a delay, $\tau_{recovery}$, between the occurrence of the gradient echo, and acquisition of the NMR spectrum ($90° - \text{PFG}_{encode} - 90° - T - 90° - \text{PFG}_{decode} - 90° - \tau_{recovery} - 90° - \text{Acquire}$). They refer to this experiment as the 'longitudinal-eddy-current-delay' or LED experiment. Solvent suppression schemes for measurement of protein signals in aqueous solution can easily be added to such schemes (Altieri et al., 1995) (Figure 1A).

A second advance made in suppressing the effect of eddy currents is the introduction of bipolar gradient pulse pairs (Wider et al., 1994), which are sets of opposite polarity PFGs, separated by a 180° radiofrequency pulse. Their incorporation into the LED experiment (Wu et al., 1995), resulted in the so-called bipolar pulse pair LED or BPP-LED pulse scheme (Figure 1B). Another potentially important improvement compensates for the effect of flow, typically caused by small temperature gradients across the sample, which can result in systematic overestimation of the diffusion constant (Xia and Callaghan, 1991; Jerschow and Muller, 1997). All our experi-

ments were carried out at room temperature, in a Shigemi microcell, and comparison of flow-compensated measurements with the regular BPP-LED experiment yielded identical results. Therefore, all subsequent experiments were carried out with the regular BPP-LED experiment.

As discussed below, the use of bipolar gradient pulses in LED experiments also has a second, more important advantage when applied to macromolecules or other large systems. Analysis of the regular LED pulse scheme (Figure 1A) shows that chemical shift evolution takes place between the first and second 90° pulses, for a total duration $\delta + 2\tau$. Consequently, magnetizations of different nuclear spins within a given molecule are stored along the $+z$ or $-z$ axis, depending on their chemical shift offsets. During the subsequent diffusion delay, T, NOE spin exchange occurs and rapidly attenuates the total stored magnetization. In contrast, for the BPP-LED experiment, chemical shift evolution during the gradient encoding period ($\delta+2\tau$) is refocused and all magnetization within a given molecule is either stored along $+z$ or $-z$, depending on its position in the sample. Therefore, to first order, NOE spin exchange effects are absent in this case, and the stored signal decays only slowly, at a rate determined by the non-selective longitudinal relaxation time.

The impact of the NOE attenuation during the diffusion delay, T, depends on the duration of the diffusion delay and on the rotational correlation time of the system investigated. For example, for a small protein such as ubiquitin (76 residues; τ_c = 4 ns), the LED and BPP-LED experiments yield identical intensities for a short (3 ms) T duration (Figure 2A), but considerable attenuation occurs for longer (400 ms) diffusion delays when comparing the LED to the BPP-LED results (Figure 2B). The NOE attenuation effect is much more pronounced for larger proteins, where NOE transfer becomes more efficient. This is illustrated by a similar comparison made for the M2 peptide, anchored in POPC bicelles (200 mg/ml; q = 0.15). A gradient-based coherence selection scheme is used to suppress the strong signals from both the water and the detergent and POPC (Figure 1C) (Kay et al., 1992a). Comparison of the LED and BPP-LED versions of this experiment shows that the amide signals of the two ^{15}N-labeled residues (Ala[7] and Gly[12]) have completely decayed in the LED experiment, but retain nearly full intensity (except for the effects of diffusion decay, transverse relaxation during the INEPT and Rance-Kay periods, and non-selective longitudinal re-

laxation during the diffusion delay) in the BPP-LED version (Figure 2C). All experiments reported below were therefore carried out with the BPP version of the LED experiment. Note, however, that the attenuation resulting from NOEs during a fixed diffusion delay is the same for weak and strong gradients. So, NOE attenuation only affects the signal-to-noise of the diffusion measurement and does not introduce systematic errors in the regular LED experiment. Therefore, measurements made in our study with the BPP-LED experiments can be compared directly to earlier results from LED.

Concentration dependence of D_s

At low volume fractions, $\Phi \leq 0.15$, the concentration dependence of the long-term self-diffusion coefficient of particles in water is, to a good approximation (Tokuyama and Oppenheim, 1994), given by

$$D_s = D_0(1 - 3.2\lambda\Phi), \qquad (2)$$

where D_s is the measured self-diffusion coefficient, D_0 is the single particle self-diffusion coefficient at infinite dilution, and $\lambda = 1$ for hard-sphere, non-interacting particles. For our studies, the dry volume fraction, Φ, is known from the specific density and weight fraction of the phospholipids and detergents. In the dilute limit ($\Phi \leq 0.15$), measurement of D_s as a function of concentration yields a straight line whose intercept at $\Phi = 0$ corresponds to D_0. The D_0 value can be used directly in the Stokes-Einstein relation,

$$D_0 = kT/(6\pi\eta R_H), \qquad (3)$$

to obtain the hydrodynamic radius, R_H. For oblate ellipsoid particles, D_0 is smaller by the shape factor, F, compared to spherical particles of the same volume (Cantor and Schimmel, 1980):

$$F = (p^2 - 1)^{1/2}/\{p^{2/3} \tan^{-1}[(p^2 - 1)^{1/2}]\}, \qquad (4)$$

where p is the aspect ratio. For the bicelles under study ($q \leq 0.5$), the refined Vold-Prosser model (Vold and Prosser, 1996; Glover et al., 2001) indicates that $p \leq 2$. For such small aspect ratios, the effect of the shape factor is very small. For example, for an oblate ellipsoid with $p = 2$, Eq. 4 indicates $F = 1.042$.

Lysozyme

For calibration purposes and to test validity of Equation 2, measurements were carried out on HEW lysozyme. For compatibility with previous results, these

Table 1. Diffusion constants, D_0, unhydrated radii R, interaction volume scale factors, λ, and derived mass of the unhydrated micelle for various bicelle and micelle samples[a]

Sample	q	D_0 $(10^{-11}$ m^2 s$^{-1})$	R[b] (Å)	λ	Mass[c] (kD)
Lysozyme	–	11.54[d]	16.0[e]	1.10 ± 0.05	14.3[e]
DHPC	0	11.22	16.5	1.30 ± 0.05	12.3
DMPC/DHPC	0.15	9.23	20.0	0.95 ± 0.05	21.7
DMPC/DMPS/DHPC[f]	0.15	9.27	19.8	*g*	21.1
POPC/DHPC	0.15	9.00	20.5	0.95 ± 0.05	23.4
POPC/POPG/DHPC[h]	0.15	9.03	20.4	*g*	23.1
POPC/DHPC + M2[i]	0.15	8.60	21.5	0.96 ± 0.05	27.0
POPC/DHPC + M2[j]	0.30	8.14	22.7	0.98 ± 0.05	31.8
POPC/DHPC	0.53	6.34	29.1	0.95 ± 0.10	67.2
16:0 Lyso PG	–	6.62	27.9	1.24 ± 0.05	64.6

[a]Diffusion constant derived from extrapolation to infinite dilution, at 27 °C in 90/10% H$_2$O/D$_2$O. Random error is ≤ 1%, but systematic errors may be substantially larger.
[b]Radius calculated from D_0 using $R = (D_0^{\text{lysozyme}}/D_0)R_{\text{lysozyme}}$
[c]Apparent mass of the unhydrated micellar aggregate.
[d]Value scaled to account for solvent viscosity difference between 298 and 300 K.
[e]Value derived from the known molecular weight and assuming a density of 1.4 g/ml.
[f][DMPC]:[DMPS]:[DHPC] = 3:1:26.7
[g]Measurements carried out at 200 mg/ml; D_0 and R values derived assuming $\lambda = 0.95$.
[h][POPC]:[POPG]:[DHPC] = 3:1:26.7
[i][POPC]:[DHPC]:[M2 peptide] = 1 : 6.7 : 0.013; D_0 value measured for peptide H^N.
[j][POPC]:[DHPC]:[M2 peptide] = 1 : 3.3 : 0.008; D_0 value measured for peptide H^N.

measurements were carried out at 298 K. D_0 was found to be 11.1 × 10^{-11} m^2/s, and a value of 10.9 × 10^{-11} m^2/s was found for a sample concentration of 8 mg/ml, in excellent agreement with previous measurements (Altieri et al., 1995; Ilyina et al., 1997). The concentration dependence of D_S is found to be highly linear over the range of 8–120 mg/ml (Figure 4). Using a specific density of 1.4 g/ml, the concentration dependence of D_S is best fit to Eq. 2 by linear regression, yielding $D_0 = 11.1 \times 10^{-11}$ m^2 s^{-1}, and $\lambda = 1.10$. Using $\eta = 0.89$ cP, Eq. 3 indicates a hydrated volume of 45 nm^3, far larger than the volume of the protein alone (17 nm^3). This degree of hydration is also much larger than what typically is observed when deriving the hydrated volume from the rotational correlation time, extracted from either fluorescence anisotropy decay or backbone ^{15}N relaxation studies. For this reason, volumes are frequently simply extracted from the ratio of the D_0 values, using a measurement on a suitable standard as a reference (Ilyina et al., 1997). In our work, we adopt this approach herein, using the well-characterized lysozyme protein as the reference. The small change in viscosity at 300 K relative to the experimental number measured at 298 K corresponds to an increase in the lysozyme D_0 value to 11.5 × 10^{-11} m^2/s (Table 1).

DHPC micelles

Above the critical micelle concentration (C_{crit}) of DHPC, there is fast exchange between monomeric DHPC and micellar aggregates. In a simplified model, where detergent is either monomeric or part of a fixed-size micelle, the NMR-derived diffusion measurement yields the weighted average:

$$D_s = D_m(C_{\text{total}} - C_{\text{free}})/C_{\text{total}} + D_f C_{\text{free}}/C_{\text{total}}, \quad (5)$$

where C_{total} and C_{free} are respectively the total DHPC concentration and that of the free DHPC, D_m is the diffusion coefficient of the micelle, and D_f is the diffusion coefficient for monomeric, free DHPC. Its diffusion obstruction, caused by the presence of the micelles, is given by (Johannesson and Halle, 1996):

$$D_f = D_f^0/(1 + \Phi/2), \quad (6)$$

where Φ is the hydrodynamic volume fraction of the micelles, and D_f^0 is the diffusion coefficient in the absence of obstruction, i.e., below the critical micelle concentration, C_{crit}. For a DHPC sample at 5 mM,

three-fold lower than C_{crit}, we find $D_f^0 = 43.8 \times 10^{-11}$ m^2 s^{-1}. For $C_{total} > C_{crit}$: $C_{free} = C_{crit}$, whereas for $C_{total} < C_{crit}$: $C_{free} = C_{total}$.

The measured concentration dependence of D_s is shown in Figure 3 as open circles. At low DHPC concentration, the C_{free} to $C_{total} - C_{free}$ ratio depends on C_{total} in a highly non-linear fashion, which is reflected in the non-linear dependence of D_s on C_{total} (Figure 3). According to Equation 2, D_m depends linearly on $C_{total} - C_{free}$, and since C_{total} is known, the value of C_{free} can be adjusted such that D_m *versus* ($C_{total} - C_{free}$) becomes linear. This yields $C_{free} = 14.0 \pm 1$ mM, in good agreement with the critical micelle concentration literature value of 15 mM (Burns et al., 1982). Using the linear relation of D_m *versus* $C_{total} - C_{free}$ (filled circles in Figure 3), the micelle diffusion coefficient extrapolated to zero concentration is found to be 11.2×10^{-11} m^2 s^{-1}, which corresponds to a radius that is about 3% larger than that of the lysozyme reference.

The linear correlation shown in Figure 3, obtained after subtracting the contribution from monomeric DHPC to the observed self-diffusion rates, equals $D_m = D_0(1 - 3.77\, C_m)$, where $C_m = C_{total} - C_{free}$ corresponds to the micelle weight fraction. Using a density of 1.1 g/cm^3 (Tausk et al., 1974; Lin et al., 1986), this corresponds to $\lambda = 1.30$ in Equation 2, or an interaction volume that is somewhat larger than the true volume, analogous to what was seen for lysozyme.

Using the reference volume of lysozyme (17 nm^3), the volume of the DHPC micelle is calculated to be 18.5 nm^3. Based on the DHPC density, its molecular volume equals 0.687 nm^3. This results in an average aggregation number of 27, which is intermediate between the value of 35 obtained from light scattering and ultracentrifugation data (Tausk et al., 1974), and a value of 19±1 derived from small angle neutron scattering (Lin et al., 1986). Interestingly, the neutron scattering data indicate the micelle to be a prolate ellipsoid, with an aspect ratio of about 1.6, and a hydrated volume of 40 nm^3. The pairwise interaction volume, derived from the concentration dependence of the scattering intensity profile, was reported as 70 nm^3. This latter value is close to the interaction volume, $\lambda\, V = 64$ nm^3, derived from the concentration dependence of the self diffusion rate, using Equations 2 and 3.

Lyso PG micelles

The analysis described above for DHPC is also carried out for a sample of 16:0 Lyso PG, a single chain phospholipid that forms micelles. In this case, the critical micelle concentration is found to be very low, 0.05 ± 0.02 mM, close to the literature value of 0.018 mM for 16:0 Lyso PG in 0.1 M Tris-Hcl (Stafford et al., 1989). The self-diffusion coefficient, radius, and apparent mass are reported in Table 1. Again, linear dependence of D_m on the weight fraction is found (Figure 4). Fitting of the data yields $D_0 = 6.6 \times 10^{-11}$ m^2 s^{-1}, and $\lambda = 1.24$ (using a specific density of 1.18 g/cm^3). Using the lysozyme data as a reference, this corresponds to a dry volume of 91 nm^3, or a radius of 27.9 Å, and an aggregation number of *ca.* 125.

POPC/DHPC bicelles

For POPC/DHPC bicelles, non-overlapping resonances are available in the ^{1}H spectrum (at 2.00 and 0.84 ppm for POPC, and at 0.89 ppm for DHPC). Considering that the concentration of free, monomeric POPC is essentially zero, the diffusion coefficient of the bicelle (D_m) directly equals the value measured for POPC. For DHPC, D_{obs} again is the average of the bicelle-bound and monomeric forms. With the values of D_m and D_f already known, the amount of free DHPC can be calculated from Equations 5 and 6.

The amount of free DHPC is expected to depend on the molar ratio, q, of POPC *versus* DHPC, and on the POPC concentration. For $q = 3$, a free DHPC concentration, [DHPC]$_{free}$, of *ca* 5 mM has previously been reported for DMPC/DHPC bicelles (for [DMPC] = 60 mM) (Ottiger and Bax, 1998; Ramirez et al., 2000), and slightly higher (7 mM) for lower q values and lower DMPC concentrations (Glover et al., 2001). [DHPC]$_{free}$ must approach its critical micelle concentration of ~15 mM for $q \rightarrow 0$. Experimentally, our diffusion measurements yield [DHPC]$_{free}$ = 11±2 mM for $q = 0.15$, [DHPC]$_{free}$ = 9±2 mM for $q = 0.30$, and [DHPC]$_{free}$ = 7±2 mM for $q = 0.53$, all carried out at [POPC] = 53 mM. Knowledge of [DHPC]$_{free}$ is important when studying the concentration dependence of the bicelle diffusion rate, needed for extracting the extrapolated diffusion rate at zero concentration. In order to keep the value of q_{eff} approximately constant, all dilutions of POPC bicelles were carried out using a solution containing 7 mM DHPC.

Using such a dilution protocol, the dependence of D_m on the bicelle concentration is found to be highly

linear for all bicelle mixtures investigated (Figure 4). Extrapolation to zero concentration then yields their unobstructed diffusion coefficients, from which their radii can be extracted using lysozyme as a reference. Results are summarized in Table 1.

POPC/DHPC/M2 bicelles

Diffusion rates were also measured in the presence of the M2 peptide. Relative POPC:M2 molar ratios were 77:1 for $q = 0.15$; 125:1 for $q = 0.3$; 167:1 for $q = 0.53$. For the $q = 0.15$ and $q = 0.3$ samples, translational diffusion rate measurement on the ^{15}N-edited amide resonances of the peptide (using the pulse scheme of Figure 1C) yielded rates about 5% slower than those measured for POPC in the same sample (data not shown). This difference presumably reflects the fact that the fraction of bicelles containing an M2 peptide is diffusing slower than the average over bicelles with and without peptide, which is monitored by the POPC diffusion. For the $q = 0.53$ sample, the amide proton line width was large, and consequently the signal-to-noise ratio was too low for measurement of the peptide diffusion rate. For the $q = 0.15$ sample with peptide, the diffusion rate was nearly 5% slower than for the corresponding sample without peptide (Table 1), indicating that the peptide increases the hydrodynamic volume of the bicelle by about 15%, roughly compatible with the added mass of a single peptide molecule.

The POPC diffusion constant in the $q = 0.53$ POPC/DHPC bicelles in the absence of M2 peptide indicates a radius of 29.1 Å, corresponding to a volume of 104 nm^3 or a mass of about 67 kD (Table 1). Considering that a POPC bilayer thickness is about 42 Å, a spherical model is unrealistic and, to a first approximation, the micelle may be modeled as an oblate spheroid. For the same volume and a thickness of 42 Å, its diameter then is 68.5 Å, corresponding to an aspect ratio of p $\approx$ 1.5. Modeling the particle as a hemitoroidal disk yields a slightly smaller aspect ratio. For such small aspect ratios, the shape factor, F (Equation 4), is so close to unity that it does not significantly (<5%) impact the volume derived from the diffusion data.

Rotational diffusion of POPC/DHPC bicelles

The high degree of internal mobility of the phospholipid molecules in a bicelle-peptide aggregate makes it difficult to estimate a reliable global rotational correlation time on the basis of their relaxation properties.

Instead, we monitor the ^{15}N relaxation rates of a water-insoluble peptide, tightly anchored to the bicelles, to obtain a measure for rotational diffusion of the micelle-peptide aggregate. The peptide used in our study is homologous to the M2 peptide that has been studied extensively both by solid state NMR and a range of other biophysical techniques. It is believed to be α-helical, with its axis traversing the POPC bilayer (Kovacs et al., 2000; Tian et al., 2002).

^{15}N T_1 and T_2 relaxation times of the two ^{15}N-enriched amides in the helical region of the peptide are listed in Table 2. Assuming the absence of internal motions on an intermediate time scale, these rates can be used in the standard manner to obtain an estimate for their rotational correlation times (Kay et al., 1989; Cavanagh et al., 1996). ^{15}N relaxation time measurements were carried out both for $q = 0.15$ and $q = 0.30$ POPC/DHPC bicelles and indicate peptide τ_c values of about 20 and 25 ns, respectively, with only a relatively weak dependence on the concentration of the bicelles (Table 2). These numbers are comparable to what is observed for proteins in the 40–50 kD range. Accounting for the difference in specific density between bicelles and proteins, this corresponds to bicelles in the 31–38 kD range, which is about 15–20% larger than the mass derived from translational diffusion data recorded on the same peptide-bicelle systems (Table 1).

Concluding remarks

Pulsed field gradient measurements of translational diffusion rates yield a convenient measure to probe the size of various micelles and mixed micelles. However, as these measurements are often carried out at considerably higher concentrations than what is used for analogous measurements on proteins, it is particularly important that the concentration dependence is taken into account when interpreting the results.

As has previously been noted for proteins, the absolute hydrodynamic volume derived from translational diffusion using Equation 3 considerably exceeds the dry volume. For this reason, only when using a reference compound, such as lysozyme in our study, is the DHPC micelle size obtained from translational diffusion in agreement with that obtained from other biophysical techniques. This result suggests that the hydrodynamic volume applicable for translational diffusion is more than two-fold larger than the dry volume, both for proteins and detergent micelles. A

Table 2. [15]N relaxation times for Ala[7] and Gly[12] residues of the M2 peptide in POPC/DHPC bicelles

Concentration[a]	T_1 (ms)	T_2 (ms)	τ_c (ns)	T_1 (ms)	T_2 (ms)	τ_c (ns)[b]
$q = 0.15$	Ala[7]			Gly[12]		
20	1342	37	22.0	1348	41	20.9
11	1267	41	20.2	1257	42	19.9
7	1258	40	20.4	1281	45	19.4
$q = 0.30$						
20	1411	25	27.6	1419	27	26.6
11	1670	33	26.1	1702	37	24.8
7	1366	31	24.3	1381	33	23.7

[a]The numbers in the first column represent the weight percentage of phospholipid in each sample.
[b]τ_c is derived from T_1 and T_2 assuming isotropic rotational diffusion.

similar ratio between the hydrated and 'dry' volumes of DHPC micelles was observed by small angle neutron scattering (Lin et al., 1986). When determining protein volume from rotational diffusion, using ^{15}N relaxation times, the ratio between the hydrated and dry volumes tends to be much closer to unity, and the reason for this discrepancy is currently not understood. So, even though reasonable particle volumes are derived from translational diffusion rates when using a reference compound such as lysozyme, errors in the derived dry mass will be introduced for samples that have a hydrated versus dry volume ratio that differs from that of the reference compound.

The ability to monitor simultaneously the translational diffusion rates for short and long chain phospholipids in mixed micelles or bicelles provides another convenient tool to estimate the concentration of free, monomeric detergent. Results we obtained in this manner are in good agreement with literature data derived in a variety of different ways (Ottiger and Bax, 1998; Ramirez et al., 2000; Glover et al., 2001). The concentration dependence of the translational diffusion rate of DHPC micelles also yields an accurate measure of the critical micelle concentration.

The large hydrodynamic volume observed for DHPC micelles, both by our self-diffusion measurements and previous neutron scattering data (Lin et al., 1986), points to a very loose packing of the headgroups, with a large amount of water interspersed between them. Our data on lyso-PG indicate that for these micelles the head-group packing must be even looser. It is likely that this poor packing in the outer shell of the micelle results from geometric constraints when attempting to bury the lipophilic hydrocarbon tails in a small spherical volume. The size

of lyso-PG micelles, derived from our diffusion experiments, is much larger than indicated by the favorable relaxation properties and spectral characteristics of peptides anchored to such micelles (Krueger-Koplin et al., 2004). This indicates considerable mobility of the bound peptide or protein relative to this large micelle. We therefore speculate that the loose packing near the lyso-PG micelle surface, combined with the moderate viscosity of its hydrocarbon core, are the primary factors responsible for this extensive mobility. For the M2 peptide anchored in DHPC/POPC bicelles the opposite is observed: the ^{15}N relaxation properties correspond to a rotational correlation time that is slightly longer than what is expected for a system of the diffusion-derived volume. This indicates that, at least for a helical peptide that traverses the bicelle bilayer, mobility of the peptide relative to the phospholipid bicelle does not significantly improve the relaxation characteristics of the amide sites on the transmembrane helix. On the other hand, the small difference between the effective volumes derived using the two approaches may result from deviations of the above discussed assumption that the fractional hydration volume of the peptide-bicelle aggregate is identical to that for lysozyme.

References

Altieri, A.S., Hinton, D.P. and Byrd, R.A. (1995) *J. Am. Chem. Soc.*, **117**, 7566–7567.

Burns, R.A., Roberts, M.F., Dluhy, R. and Mendelsohn, R. (1982) *J. Am. Chem. Soc.*, **104**, 430–438.

Cantor, C.R. and Schimmel, P.R. (1980) *Biophysical Chemistry*, Vol. Part 2, Freeman, San Francisco.

Cavanagh, J., Fairbrother, W.J., Palmer, A.G. and Skelton, N.J. (1996) *Protein NMR Spectroscopy: Principles and Practice*, Academic Press, San Diego.

Chou, J.J., Kaufman, J.D., Stahl, S.J., Wingfield, P.T. and Bax, A. (2002) *J. Am. Chem. Soc.*, **124**, 2450–2451.

Fernandez, C., Hilty, C., Wider, G. and Wüthrich, K. (2002) *Proc. Natl. Acad. Sci. U.S.A.*, **99**, 13533–13537.

Gaemers, S. and Bax, A. (2001) *J. Am. Chem. Soc.*, **123**, 12343–12352.

Gibbs, S.J. and Johnson, C.S. (1991) *J. Magn. Reson.*, **93**, 395–402.

Glover, K.J., Whiles, J.A., Wu, G.H., Yu, N.J., Deems, R., Struppe, J.O., Stark, R.E., Komives, E.A. and Vold, R.R. (2001) *Biophys. J.*, **81**, 2163–2171.

Holz, M. and Weingartner, H. (1991) *J. Magn. Reson.*, **92**, 115–125.

Ilyina, E., Roongta, V., Pan, H., Woodward, C. and Mayo, K.H. (1997) *Biochemistry*, **36**, 3383–3388.

Jerschow, A. and Muller, N. (1997) *J. Magn. Reson.*, **125**, 372–375.

Johannesson, H. and Halle, B. (1996) *J. Chem. Phys.*, **104**, 6807–6817.

Kay, L.E., Keifer, P. and Saarinen, T. (1992a) *J. Am. Chem. Soc.*, **114**, 10663–10665.

Kay, L.E., Nicholson, L.K., Delaglio, F., Bax, A. and Torchia, D.A. (1992b) *J. Magn. Reson.*, **97**, 359–375.

Kay, L.E., Torchia, D.A. and Bax, A. (1989) *Biochemistry*, **28**, 8972–8979.

Knubovets, T., Osterhout, J.J., Connolly, P.J. and Klibanov, A.M. (1999) *Proc. Natl. Acad. Sci. U.S.A.*, **96**, 1262–1267.

Korzhnev, D.M., Skrynnikov, N.R., Millet, O., Torchia, D.A. and Kay, L.E. (2002) *J. Am. Chem. Soc.*, **124**, 10743–10753.

Kovacs, F.A., Denny, J.K., Song, Z., Quine, J.R. and Cross, T.A. (2000) *J. Mol. Biol.*, **295**, 117–125.

Krueger-Koplin, R.D., Sorgen, P.L., Krueger-Koplin, S.T., Rivera-Torres, I.O., Cahill, S.M., Hicks, D.B., Grinius, L., Krulwich, T.A. and Girvin, M.E. (2004) *J. Biomol. NMR*, **28**, 43–57.

Lin, T.L., Chen, S.H., Gabriel, N.E. and Roberts, M.F. (1986) *J. Am. Chem. Soc.*, **108**, 3499–3507.

Lin, T.L., Liu, C.C., Roberts, M.F. and Chen, S.H. (1991) *J. Phys. Chem.*, **95**, 6020–6027.

Luchette, P.A., Vetman, T.N., Prosser, R.S., Hancock, R.E.W., Nieh, M.P., Glinka, C.J., Krueger, S. and Katsaras, J. (2001) *Biochim. Biophys. Acta-Biomembr.*, **1513**, 83–94.

Mills, R. (1973) *J. Phys. Chem.*, **77**, 685–688.

Nieh, M.P., Glinka, C.J., Krueger, S., Prosser, R.S. and Katsaras, J. (2001) *Langmuir*, **17**, 2629–2638.

Ottiger, M. and Bax, A. (1998) *J. Biomol. NMR*, **12**, 361–372.

Price, W.S. (1997) *Concept. Magn. Reson.*, **9**, 299–336.

Ramirez, B.E., Voloshin, O.N., Camerini-Otero, R.D. and Bax, A. (2000) *Protein Sci.*, **9**, 2161–2169.

Stafford, R.E., Fanni, T. and Dennis, E.A. (1989) *Biochemistry*, **28**, 5113–5120.

Stejskal, E.O. and Tanner, J.E. (1965) *J. Chem. Phys.*, **42**, 288–292.

Tanner, J.E. (1970) *J. Chem. Phys.*, **52**, 2523–2526.

Tausk, R.J.M., van Esch, J., Karmiggelt, J., Voordouw, G. and Overbeek, J.T.G. (1974) *Biophys. Chem.*, **1**, 184–203.

Tian, C.L., Tobler, K., Lamb, R.A., Pinto, L.H. and Cross, T.A. (2002) *Biochemistry*, **41**, 11294–11300.

Tokuyama, M. and Oppenheim, I. (1994) *Phys. Rev. E*, **50**, R16–R19.

Vold, R.R. and Prosser, R.S. (1996) *J. Magn. Reson. Ser. B*, **113**, 267–271.

Vold, R.R., Prosser, R.S. and Deese, A.J. (1997) *J. Biomol. NMR*, **9**, 329–335.

Wider, G., Dotsch, V. and Wüthrich, K. (1994) *J. Magn. Reson. Ser. A*, **108**, 255–258.

Wu, D.H., Chen, A.D. and Johnson, C.S. (1995) *J. Magn. Reson. Ser. A*, **115**, 260–264.

Xia, Y. and Callaghan, P.T. (1991) *Macromolecules*, **24**, 4777–4786.